Journal Pre-proof

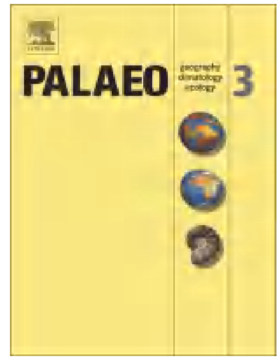

Re-examination of Dashanpusaurus dongi (Sauropoda: Macronaria) supports an early Middle Jurassic global distribution of neosauropod dinosaurs

Xin-Xin Ren, Shan Jiang, Xu-Ri Wang, Guang-Zhao Peng, Yong Ye, Lei Jia, Hai-Lu You

PII: S0031-0182(22)00489-8

DOI: https://doi.org/10.1016/j.palaeo.2022.111318

Reference: PALAEO 111318

To appear in: *Palaeogeography, Palaeoclimatology, Palaeoecology*

Received date: 28 September 2022

Revised date: 10 November 2022

Accepted date: 10 November 2022

Please cite this article as: X.-X. Ren, S. Jiang, X.-R. Wang, et al., Re-examination of Dashanpusaurus dongi (Sauropoda: Macronaria) supports an early Middle Jurassic global distribution of neosauropod dinosaurs, *Palaeogeography, Palaeoclimatology, Palaeoecology* (2022), https://doi.org/10.1016/j.palaeo.2022.111318

Re-examination of *Dashanpusaurus dongi* (Sauropoda: Macronaria) supports an early Middle Jurassic global distribution of neosauropod dinosaurs

Xin-Xin Ren[a*], Shan Jiang[b,c,d], Xu-Ri Wang[a], Guang-Zhao Peng[b,c,d], Yong Ye[b,c,d], Lei Jia[e], Hai-Lu You[f,g,h*]

[a]Key Laboratory of Stratigraphy and Paleontology of the Ministry of Natural Resources, Institute of Geology, Chinese Academy of Geological Sciences, Beijing 100037, China

[b]Zigong Dinosaur Museum, Zigong 643013, China

[c]Research Center of the Jurassic Stratigraphy and Paleontology, Zigong Dinosaur Museum, Zigong, China;

[d]Key Laboratory of Paleontology and Paleoenvironment Coevolution (Sichuan-Chongqing Joint Construction), Zigong, China;

[e]Shanxi Museum of Geology, Taiyuan 030024, China

[f]Key Laboratory of Vertebrate Evolution and Human Origins, Institute of Vertebrate Paleontology and Paleoanthropology, Chinese Academy of Sciences, Beijing 100044, China

[g]CAS Center for Excellence in Life and Paleoenvironment, Beijing 100044, China

[h]College of Earth and Planetary Sciences, University of Chinese Academy of Sciences, Beijing 100044, China

*Corresponding authors: Xin-Xin Ren (email: laotourenxin@126.com) and Hai-Lu You (email: youhailu@ivpp.ac.cn)

ABSTRACT

Neosauropods were the dominant sauropod clade with a global distribution as early as the Late Jurassic. However, its distribution and biogeography in the Middle Jurassic are unclear due to the paucity of phylogenetic evidence for neosauropod taxa of this age. In China, the only reported Middle Jurassic neosauropod, the diplodocoid, has challenged the traditional East Asian Isolation Hypothesis for dinosaur paleobiogeography. Here, based on phylogenetic analysis including *Dashanpusaurus dongi* from the early Middle Jurassic of southwest China, we demonstrate that this taxon represents the earliest diverging macronarian as well as the stratigraphically lowest neosauropod globally. Our biogeographic analysis together with other geological evidence further indicates that neosauropods achieved a global distribution at least in the early Middle Jurassic while Pangaea was still a coherent landmass.

Keywords: Sauropoda; Macronaria; Pangaea; Biogeography; Middle Jurassic; Lower Shaximiao Formation

1. Introduction

Sauropods were globally distributed gigantic herbivorous dinosaurs that dominated many Jurassic and Cretaceous terrestrial faunas (Upchurch et al., 2004). However, several aspects of the evolution of sauropods remain poorly understood, such as the origin of Neosauropoda and the early diversification of its major groups

(Diplodocoidea and Macronaria) (Xu et al., 2018). Nevertheless, in recent years, significant progress has been made in our understanding of Jurassic sauropod diversification and biogeography in East Asia (e.g. Xu et al., 2018; Mannion et al., 2019). For example, the origination times of major neosauropod clades and their existence in East Asia are far earlier than previously realized, although sampling biases make the diversity still cryptic (Xu et al., 2018); while the predominantly East Asian non-neosauropodan clade, Mamenchisauridae, traditionally thought to constitute endemic radiations has been reported not only exists in East Asia during the Middle Jurassic (Mannion et al., 2019; Moore et al., 2020). These advances encourage and urge us to revisit Middle Jurassic materials that were previously discovered, such as those from the Zigong Dashanpu quarry in southwest China.

Dashanpusaurus dongi was first reported as a camarasaurid sauropod by Peng et al. (2005). Its horizon is situated at the base of the Lower Shaximiao Formation. Here, we re-examine the anatomy of its materials and include it in phylogenetic analysis for the first time. We demonstrate that it is, to our knowledge, the earliest diverging macronarian as well as the earliest known neosauropod by geological age. Our biogeographic analysis including this discovery further calibrates the timing of neosauropod diversification and undermines the Jurassic East Asian Isolation Hypothesis (EAIH).

2. Materials and Methods

Materials.

The two specimens assigned to this taxon include the holotype (ZDM 5028) and the paratype (ZDM 5027). The two partly articulated skeletons derive from a single locality (Dashanpu quarry) in the Lower Shaximiao Formation of Zigong, southern Sichuan, China. The holotype (ZDM5028) of the taxon is including near complete middle-posterior cervical to posterior caudal vertebrae, left ulna, ilium, pubis, femur, and tibia. By contrast, the paratype (ZDM 5027) includes four anterior cervical vertebrae, a nearly complete dorsal series, left humerus, and radius.

Phylogenetic analysis. We have scored the two specimen-level operational taxonomic units (OTUs) and 'Dashanpusaurus Total', for the data matrix of Ren et al. (2020) (Supplementary Data (SD) 2 to 5). The original version of this matrix comprises 386 characters scored for 76 sauropodomorph taxa. We have chosen to use this matrix as the main dataset based on the matrix of Xu et al. (2018), which is the up-to-date version of the series of datasets produced by Carballido and colleagues, and includes scores for many Middle-Late Jurassic neosauropods (e.g. Middle Jurassic *Lingwulong* from China), and many mamenchisaurids (e.g. *Omeisaurus tianfuensis*, and *Mamenchisaurus youngi*). Furthermore, this dataset is suitable for our study because it samples a phylogenetically and spatiotemporally wide array of sauropodomorph taxa, and thus gives *Dashanpusaurus* the freedom to cluster anywhere within known sauropod diversity. Nine taxa were added to the matrix (including *Dashanpusaurus dongi*, *Atlasaurus imelakei*, *Lourinhasaurus alenquerensis*, *Omeisaurus puxiani*, *Spinophorosaurus nigerensis*, *Wamweracaudia keranjei*, *Rhoetosaurus brownei*, *Aragosaurus ischiaticus*, and *Janenschia robusta*), with 386 original characters plus 14 new characters. Coding of the characters for these taxa is based on an extensive review of the literature (e.g. Longman, 1926; Monbaron et al., 1999; Bonaparte et al., 2000; Remes et al., 2009; Carudo et al., 2012; Nair and Salisbury, 2012; Mocho et al., 2014; Royo-Torres et al., 2014; Mannion et al., 2019; Vidal et al., 2020), as well as our personal observations.

Phylogenetic analyses were carried out in TNT v. 1.5 (Goloboff et al., 2008) (SD 2-5). Equal weights parsimony (EWP) and extended implied weighting (EIW) analyses are employed in the phylogenetic analysis. For extended implied weighting analyses, we used a concavity constant (K) of 12 (referred to Moore et al., 2020). The New Technology Search was applied first, 50 search replications were used as a starting point for each hit, and with the consensus stabilized 10 times, using random and constraint sectorial searches under default settings, five ratchet iterations, and five rounds of tree fusing per replicate (‘xmult=replications 50 hits 10 css rss ratchet 5 fuse 5’). The resulting MPTs were then used as the starting trees for a Traditional Search using TBR. The support for each node in the trees was assessed in TNT using GC values generated via symmetric resampling, based on 5000 replicates. The latter analyses used the Traditional Search option with TBR. Character mapping was carried out in Mesquite version 2.75 (Maddison and Maddison, 2011).

Biogeographic analysis. The biogeographic analyses in this study have generally followed the operation of Xu et al. (2018). We added some 'new' taxa and revised some taxon ages. The 84 taxa in the agreement subtree have been dated generally using the data of Xu et al., (2018). The taxon ages of the original literature were derived from the Paleobiology Database (https://www.paleobiodb.org/) and Fossilworks Database (http://fossilworks.org/?a=home), as well as the primary literature. The ages of several Jurassic stratigraphic units from China are in a state of flux. Indeed, this is the case for the Shaximiao Formation. Wang et al. (2018) recently dated it as Oxfordian, rather than the Middle Jurassic (Bajocian-Callovian) age, which had been the traditional consensus for a long time (e.g. Zhang et al., 1976; Chen et al., 1982; Shen, 2003, 2004, 2010; Liao et al., 2014). Although our taxon ages are generally dated from the latest literature, in this case, our ages differ from Wang et al. (2018), so we use our data in this study. Here, the added taxa, such as *Yuanmousaurus*, from the Middle Jurassic Zhang Formation (Aalenian-Callovian) of Southwest China, are known from a single specimen from a single horizon, so their range of First Appearance Datum (FAD) and Last Appearance Datum (LAD) values lack temporal resolution rather than a stratigraphic range. Thus, these taxa were given midpoint ages, as in other recent studies (e.g. Xu et al., 2018; Mannion et al., 2019). The revised taxa include multiple specimens from a single horizon, such as *Lingwulong*, the bone-bearing stratigraphic unit is revised from Yan'an Formation to Zhiluo Formation, making the stratigraphic age for the quarries revised from early Middle Jurassic

(Aalenian) to middle-late Middle Jurassic (Bathonian-Callovian) according to the newest literature (You et al., 2019), are given midpoint ages for the FAD and LAD. Some monophyletic taxa, such as *Omeisaurus*, are known from multiple specimens at several stratigraphic horizons, are divided as separate OTUs and given a stratigraphic range and so have different FAD and LAD. The added and revised taxon ages listed in this study referring the 2020 version of the International Commission on Stratigraphy Chronostratigraphic Chart (Cohen et al., 2013). The FADs, LADs, and midpoint ages for the 84 taxa used in the biogeographic analysis are given in Supplementary Data 10.

We used the R package BioGeoBEARS (see also: Gorscak and O'Connor, 2016; Poropat et al., 2016; Xu et al., 2018; Mannion et al., 2019) to analyze the biogeographic history of sauropods to estimate the areas occupied at ancestral nodes (see Supplementary Data 16 for R script). These analyses require a fully resolved and dated phylogenetic topology (see Supplementary Data 9). Iterative PCR was used in TNT to identify unstable OTUs. We get the unstable OTU (Calcareo Diplodocid) in this study, then we removed this unit to get a fully resolved topology. This taxon was dated using the Paleobiology Database (https://paleobiodb.org/), with modifications based on the primary and recent literature. All taxon ages were converted into absolute ages, using the 2020 version of the International Commission on Stratigraphy Chronostratigraphic Chart (https://www.iugs.org/ics). The EWP was calibrated against time using the R package strap (Bell and Lloyd, 2015), via the Date Phylo command.

The root length was set at 5 million years, and adjacent zero-length branches were distributed using the ‘equal’ method (see also: Brusatte et al., 2008). BioGeoBEARS uses Maximum Likelihood to enable ancestral area estimation (Matzke, 2013, 2014). Six different models (DEC, DEC+J, DIVALIKE, DIVALIKE+J, BAYAREALIKE, and BAYAREALIKE+J. DEC and DIVALIKE) of how the geographic ranges occupied by ancestors and lineages might evolve on a tree are implemented. These models allow different forms of vicariance to occur at nodes, whereas BAYAREALIKE disallows vicariance, and instead constrains daughter lineages to inherit the range of their immediate ancestor (Matzke, 2013). The +J versions of each model share the same properties as their non-J versions, except that the former also allows founder-event speciation to occur at ancestral nodes (i.e. long-distance geodispersal). Log-likelihood ratio tests and AIC values are then used to determine which of these models best fits the data. In this study, we allowed each ancestor to occupy up to the full eight geographic areas available. We ran two analyses, using the relaxed and harsh versions of our dispersal multiplier matrices applied to the dated EWP agreement subtrees. BioGeoBEARS was run in R version 3.2.3 (R Core Development Team, 2015), and the script used is presented in Supplementary Data 16.

Anatomical abbreviations

AL, accessory lamina contacting the perzygodiapophyseal lamina and paraodiapophyseal lamina; **ap**, accessory process; **CPRL**, centroprezygapophyseal lamina; **di**, diapophysis; **dpc**, deltopectoral crest; **EPRL**, epipophyseal-prezygapophyseal lamina; **IE**, internal excavation; **lc**, lateral condyle;

mc, medial condyle; **nsp**, neural spine; **pa**, parapophysis; **PCDL**, posterior centrodiapophyseal lamina; **pf**, lateral pneumatic fossa; **PODL**, postzygodiapophyseal lamina; **poz**, postzygapophysis; **PRDL**, prezygodiapophyseal lamina; **prz**, prezygapophysis; **SPRL**, spinoprezygapophyseal lamina.

Other abbreviations

Aal, Aalenian; **AF**, Asia - Africa; **AN**, Asia - North America; **AS**, Asia - South America; **AFN**, Asia - Africa - North America; **ANS**, Asia - North America - South America; **AS**, Asia - South America; **Baj**, Bajocian; **Bat**, Bathonian; **Cal**, Callovian; **Fm.**, Formation; **MRCA**, the most common ancestor; **OTU**, operational taxonomic unit; **SD**, Supplementary Data.

3. Results

3.1 Systematic paleontology

Sauropoda Marsh, 1878

Neosauropoda Bonaparte, 1986

Macronaria Wilson and Sereno, 1998

Dashanpusaurus dongi Peng, Ye, Gao, Shu et Jiang, 2005

Locality and horizon

The specimens were excavated in Dashanpu Town, Zigong City, Sichuan Province, Southwest China (Fig. 1). They were recovered from purplish-red silty mudstones, situated at the bottom of the Lower Shaximiao Formation. Traditionally, the Lower Shaximiao Formation is generally considered to have been deposited in Middle Jurassic (e.g. CCMSPSB, 1982; BGMRSP, 1997; Wang et al., 2010). Some invertebrate fossil records (e.g. conchostracans) are indicative of a (potentially Bajocian to Bathonian) middle Middle Jurassic age (Zhang et al., 1976; Chen et al., 1982; Shen, 2003, 2004, 2010; Liao et al., 2014). However, obtained radiometric constraints for this formation represent another scenario. Previous electron spin resonance (ESR) dating results in the age of the Lower to Upper Shaximiao Formations were interpreted as 178 to 167 Ma (Zong and Shi, 1997; Guo et al., 2000). Then, a series of detrital zircon U-Pb geochronology for the Lower Shaximiao Formation yielded 163 ± 3 Ma (the youngest single zircon age), 160 ± 4 Ma, and 158 ± 7 Ma (weighted average age of the youngest subpopulation) (Li et al., 2010; Luo et al., 2014; Qian et al., 2016; Wang et al., 2018). In especially, Wang et al. (2018) reported the youngest inductively coupled plasma-mass spectrometry (ICP-MS) detrital zircon U-Pb age for the *Shunosaurus*-*Omeisaurus*-bearing units from Lower Shaximiao Formation is 159 ± 2 Ma, as the maximum depositional age. Additionally, a new zircon LA-ICP-MS U-Pb ages from interbedded tuffaceous siltstone collected beneath the fossil-bearing layers of Yunyang Dinosaur Fauna in northeastern Chongqing (northeastern Sichuan Basin), zircon U-Pb geochronology yielded a maximum depositional age of 166.0 ± 1.5 Ma (late Middle Jurassic) (Zhou et al., 2021). These geochronological data show that increasing amounts of radiometric dating evidence support a late Middle Jurassic to Late Jurassic depositional age for this formation. However, the plant assemblage in this formation consists of *Neocalamites-Coniopteris* from the early Middle Jurassic era and further correlates with the regional fossil-bearing stratigraphic comparison (Yang, 1987; Deng et al., 2017; Xin et al., 2018). In general, the exact age for this formation is still controversial.

In this study, we resampled sandstones from the lowest of the Lower Shaximiao Formation near the quarry of *Dashanpusaurus dongi* specimens in the Zigong Dinosaur Museum. A total of 107 zircon grains with euhedral morphologies and oscillatory zoning patterns were selected for the U-Pb dating. The U-Pb dating is conducted using an Agilent 7500 ICP-MS with an ESI NWR 193-nm laser ablation system in CDUT, following the methodology described by Zhang et al. (2019). The youngest age for the zircon sample is 166.0 ± 1.59 Ma, and weighed average ages of the youngest subpopulation under the constraints of 1σ and 2σ are 170.9 ± 0.64 Ma and 169.9 ± 0.63 Ma (Supplementary figure 1). The maximum confidence age of 169.9 ± 0.63 Ma was selected as the final result. In general, we suggest the age of the bottom of the Lower Shaximiao Formation in Dashanpu is possibly equal to/ earlier than 170 Ma (earliest Bajocian), and we provisionally suggest the age of *Dashanpusaurus dongi* could be as early as the earliest Bajocian (see Supplementary data 1 and 6).

Diagnosis

Revised autapomorphies: neural canals are sub-square in anterior dorsal vertebrae; a thin accessory lamina connects prezygodiapophyseal lamina and paradiapophyseal lamina, forming an angle of approximately 75° to the horizontal in middle dorsal vertebrae; four longitudinal ridges on the anterodistal margin of the humerus (Fig. 2). Detailed monographic description of *Dashanpusaurus* is prepared in another article (Ren et al., 2022).

3.2 Phylogenetic analyses

Our equal weights parsimony (EWP) analysis of the main dataset (SD2-5) resulted in 3 most parsimonious trees (MPTs) with a length of 1387 steps (consistency index=0.340; retention index=0.687). The result as a strict consensus is generally well-resolved, and *Dashanpusaurus dongi* was recovered within Neosauropoda as a basal member of Macronaria. Neosauropoda is supported by four unambiguous synapomorphies (‘0’ to ‘1’ for characters 96, 139, and 225; ‘0’ to ‘2’ for character 106). Macronaria is supported by nine unambiguous synapomorphies (‘0’ to ‘1’ for characters 162, 238, 283, 387, and 390; ‘1’ to ‘0’ for 136, and 393; ‘1’ to ‘2’ for character 116; ‘2’ to ‘1’ for character 394), and *Dashanpusaurus dongi* shares all the characters (height divided by width of the cervical posterior articular surface is between 0.9 and 0.7 (ch. 116); dorsal transverse processes are directed laterally or slightly upwards (ch. 136); transverse section of middle and posterior dorsal centra is slightly dorsoventrally compressed (ch. 162); acromion process lies nearly at midpoint of the acromion (ch. 238); length of puboischial contact is about the half total length of pubis (ch. 288); mediolateral width of posterior articular face to dorsoventral height ratio on the middle to posterior dorsal centra is 1.0 or greater (ch. 387); scapular acromion situated posterior to the acromial ridge forms a separate excavated area (ch. 390); neural spine minimums width/length of anterior dorsal vertebrae is 0.50 or greater (ch. 393); neural spine length of anterior dorsal vertebrae slightly higher than the centrum (ch. 394). Then, the subsequently extended implied weighting (EIW) analysis resulted in 3 MPTs with a length of 56.07553 steps (consistency index=0.340; retention index=0.687). In our EIW analysis, *Dashanpusaurus dongi* is situated at the basalmost member of Macronaria and supported by nine unambiguous character changes, the character of which are similar to that in EWP analysis.

Additionally, three non-Asian eusauropod taxa (Australian *Rhoetosaurus*, African *Spinophorosaurus* and *Wamweracaudia*) were recovered within Mamenchisauridae in our EWP and EIW analyses (Fig. 3), and the mamenchisaurid clade is supported by eight unambiguous synapomorphies (‘0’ to ‘1’ for characters 112, 198, 376, and 392; ‘1’ to ‘0’ for characters 125, 227, 305, and 377). Therein, *Spinophorosaurus* is situated as the basal-most of the mamenchisaurid clade, and is supported by all the eight characters: the ventral surface of cervical centra is transversely concave (ch. 112); the height of the neural arch of middle cervical vertebrae is less than the height of the posterior articular surface (ch. 125); transverse processes of anterior caudal neural spines are ‘wing-like’ shaped, not tapering distally (ch. 198); chevrons persisting throughout at least 80% of the tail (ch. 227); transverse breadth of femoral distal condyles is subequal (ch. 305); two accessory processes on the anterodistal end of the humerus (ch. 376); medial accessory process from the humeral anterodistal end is more robust than the lateral one (ch. 377); parapophyses of middle and posterior cervical vertebrae are anteroposteriorly elongated (ch. 392). The clade (*Rhoetosaurus* + other mamenchisaurids) is supported by two unambiguous synapomorphies ('0' to '1' for character 116; '1' to '0' for character 161): height divided by the width of cervical vertebrae is around 1.0 (ch. 116); posterior centroparapophyseal lamina (PCPL) of middle and posterior dorsal neural arches is absent (ch. 161). *Wamweracaudia* is resolved as the sister taxon to *Mamenchisaurus youngi*, supported by one unambiguous synapomorphy: morphology of articular surfaces in proximal caudal vertebral bodies is mediolaterally compressed (ch. 378).

3.3 Biogeographic analyses

The results of the log-likelihood ratio test and AIC values in both harsh and relaxed EWP analyses are presented in Table 1. In both two analyses, the log-likelihood ratio tests in our biogeographic analysis indicate the +J versions of the biogeographic models are strongly significantly, better fitting the data than other non +J versions (*p*-values range from 6.4^{e-6} to 8.7^{e-25}) (SD7-17). Furthermore, the AIC values for BAYAREALIKE + J are 11.2 (harsh) and 12.8 (relaxed) units lower than the next best-supported model (i.e., DEC+J) (Table. 1). It indicates that the BAYAREALIKE + J model can be regarded as strongly outperforming the other five models (Burnham and Anderson, 2002). These results further indicate that the biogeographic history of the sauropods in this study is best explained in terms of a mix of sympatry (because the BAYAREALIKE + J model only allows range duplication when cladogenesis occurs), early occurrences of widespread ancestral stocks followed by regional extinction, and founder-event speciation (Matzke, 2013, 2014). The lack of support for DEC, DIVALIKE, and the other five models also means that the data provide no clear evidence for continent-scale vicariance (See also: Xu et al., 2018; Mannion et al., 2019). Although this may indicate the true biogeographic process controlling the distributions of sauropods, it is possible that sampling biases, incorrect phylogenetic topology, and/ or errors in the dating of cladogenetic and palaeogeographic events, have obscured any evidence for vicariance signals. The ancestral area estimations for the best-supported models, i.e. BAYAREALIKE+J for the relaxed and harsh EWP, are shown in Supplementary Data 15-17.

The ancestral area estimations for the relaxed and harsh BAYAREALIKE+J results are generally similar and are identical for the key selected nodes discussed below. According to these results, the most probable areas occupied by the most recent common ancestors (MRCAs) for the following clades are Asia + Africa (Mamenchisauridae), Asia + North America (Neosauropoda, Diplodocoidea, and Macronaria), and Asia + South America (*Lingwulong* + later-diverging dicraeosaurids). Following the previous reasoning (e.g. Poropat et al., 2016; Xu et al., 2018; Mannion et al., 2019), we propose that these estimations indicate only part of areas occupied by the ancestral stocks, which in reality would have been widespread across Pangaea (instead of those anomalously discrete area reconstructions) by the Middle Jurassic, but sampling failures or phylogenetic results with low resolution could make those areas not shown in the ancestral area estimations.

4. Discussion

The East Asian Isolation Hypothesis (EAIH) has previously been the most accepted explanation to interpret the distinct difference between East Asian and other Pangaean terrestrial faunal lineages during the Jurassic to Early Cretaceous in the last three decades (e.g. Russell, 1993; Wilson and Upchurch, 2009; Mannion et al., 2011). This paradigm suggests the isolation of Asia resulted in the evolution of some endemic groups such as mamenchisaurid sauropods, and the absence of many sauropod lineages (e.g. diplodocoid) in East Asia during the Jurassic. This hypothesis, however, is debated, given that some authors considered the supporting evidence to be biased, such as Laurasia/eastern Asia might have been a center of diversification for dinosaur some clades (e.g. Manabe et al., 2000), the low species richness of Late Jurassic Asian sauropods may be attributed to a smaller number of fossiliferous terrestrial localities (e.g. Xing et al., 2015). Furthermore, two recent studies convincingly challenged this hypothesis (Xu et al., 2018; Mannion et al., 2019), especially the discovery of dicraeosaurid *Lingwulong* from the middle/late Middle Jurassic (Bathonian-Callovian) (the horizon was revised from Yan'an Fm. to Zhiluo Fm. (Bathonian-early Oxfordian)

(You et al., 2019)). Our study further shows the existence of macronarian *Dashanpusaurus* in the early Middle Jurassic (early Bajocian). Moreover, together with the later-diverging diplodocoid *Lingwulong*, these records strongly indicate neosauropods potentially possessed a relatively high diversity in Middle Jurassic East Asia. Moreover, another two macronarians are also known in Late Jurassic East Asia (*Bellusaurus*, though some phylogenetic results propose it outside Neosauropoda; *Daanosaurus*, phylogenetically recovered as a macronarian). Besides, *Wamweracaudia* from Late Jurassic Africa was recovered as a sister taxon of *Mamenchisaurus youngi*, reflecting the mamenchisaurids might not have been endemic to East Asia.

In our EWP and EIW analyses, Australian *Rhoetosaurus*, African *Spinophorosaurus*, and *Wamweracaudia* are recovered in the mamenchisaurid clade. Our biogeographic analyses using the Maximum Likelihood R Package BioGeoBEARS (SD9-19) show the most recent common ancestor (MRCA) in both harsh and relaxed EWP analyses of members of Mamenchisauridae is present in Africa and Asia. These ancestral area estimations furtherly suggest a more widespread distribution for the mamenchisaurid clade, rather than an endemic lineage (see also: Mannion et al., 2019). Although the estimations do not provide a clear indication for the center of the origin of mamenchisaurids, these indicate that this clade had become widespread across Asia, and Africa during the late Early to Middle Jurassic. Laurasia and Gondwana disconnected during the late Middle to Late Jurassic (e.g. Mannion et al., 2019), and mamenchisaurids should have become widespread earlier than Bajocian. In short, our study further undermines the EAIH. Wilson and Upchurch (2009) suggested that a disbanded endemic East Asian clade (in this case, Euhelopodidae, a monophyletic clade including *Euhelopus*, *Omeisaurus*, *Mamenchisaurus*, and *Shunosaurus*) can provide more, not less, evidence for the EAIH (Wilson and Upchurch, 2009), though they also pointed out that whether the breakdown of Euhelopodidae has weakened or strengthened support for vicariance is uncertain pending further quantitative biogeographic analysis. D'Emic (2012) defined the Euhelopodidae (including six Eary-Middle Cretaceous East Asian genera), but the members or even the existence of this group is still controversial (e.g. Carballido et al., 2013; Xing et al., 2015; Ren et al., 2018; Mannion et al., 2019a, 2019b; Moore et al., 2020; Upchurch et al., 2021). However, Poropat et al. (2022) suggest the similarity of the teeth between *Euhelopus* and multiple other Lower Cretaceous materials in China may partly support the notion of the endemic Asian clade. Although it differs from the clade that has been phylogenetically supported by Moore et al. (2020) with the varied position of *Euhelopus*, these hypotheses appear to support a unique sauropod group in East Asia during Late Jurassic to Early Cretaceous. Therefore, our biogeographic analysis provides a quantitative result supporting the hypothesis that neosauropods, including both macronarians and several diplodocoid lineages, were present in East Asia during the Middle and Late Jurassic. The direct body fossil evidence for this comes from the Middle Jurassic taxa (*Dashanpusaurus* and *Lingwulong*) and early Late Jurassic

Bellusaurus (Mo, 2013). This result significantly undermines the EAIH and its corollaries relating to invasion by titanosauriforms during the Cretaceous in association with marine regressions. We advocate the modified EAIH by previous researchers (e.g. Xu et al., 2018; Mannion et al., 2019) and further propose that the lack of Asian Late Jurassic titanosauriform records and the flourishing of Late Jurassic mamenchisaurids may indicate the vicariance was probably still relatively intense at least before the Early Cretaceous titanosauriforms turnover.

The origin and early diversification of Neosauropoda is one of the most controversial topics in the evolution of Sauropoda (Xu et al., 2018; Mannion et al., 2019). Middle Jurassic faunas are dominated by non-neosauropodan eusauropods globally, with few neosauropod records (Fig. 4). Phylogenetic analyses position the Middle Jurassic Africa *Atlasaurus* as the 'basal'-most member of either Diplodocoidea or Macronaria (e.g. Moore et al., 2020), or recovered it outside of Neosauropoda (e.g. Upchurch et al., 2015). As noted above, *Dashanpusaurus* is a macronarian in Bajocian of China and is potential the stratigraphically lowest neosauropod to date. Besides these, records of putative Early to Middle Jurassic neosauropod fragmentary materials have been reported, such as those in Toarcian Patagonia, Callovian UK and the European part of Russia (Carballido et al., 2017; Holwerda et al., 2019; Averianov and Zverkov, 2020). The putative titanosauriform tooth in the former report potentially indicates the origin and earliest diversity of Neosauropoda during the late Early-Middle Jurassic, and the putative Callovian neosauropod materials in the later reports further supporting neosauropod early diversification and related dispersal events. Additionally, the sea level was globally low throughout almost the entire Middle Jurassic until the disconnection of Laurasia and Gondwana (Poropat et al., 2016; Haq, 2017). It echoes with vast tectonic and sedimentological evidence such as widespread emergence, erosion, and localized deposition in the early Middle Jurassic of Europe (Zatoń et al., 2006; Zatoń and Taylor, 2009; Nielsen et al., 2010; Cortés and Gómez, 2018; Zohdi et al., 2021), as well as changes in invertebrate diversity patterns (e.g. Marcinowski and Gasiński, 2002; Ruban, 2007; Zatoń, 2011; Jain and Abdelhady, 2020). This spurred the development of large epicontinental basins around Pangaea (Dercourt et al., 1994). To a certain extent, the availability of non-marine environments has historically been understood to be the main determinant for biological diversification, dispersion, and adaptive radiation (e.g. Tiss et al., 2019). It seems logical to assume the globally low sea level created the non-marine environment boosts for possibly well-developed sauropod radiation (e.g. Neosauropoda) would have occurred in the Northern Pangea in or before Middle Jurassic. Because neosauropods were already highly diverse during the Middle Jurassic, the timing of their origin and initial diversification could be as early as the late Early Jurassic.

The MRCA of the neosauropod clade in both harsh and relaxed EWP analyses was hypothesized to have lived in Asia or North America. This indicates that clade probably originated in the early Middle Jurassic, and supports a widespread dispersal event before the disconnection between Laurasia and Gondwana as part of the near-global expansion of Neosauropoda in the Late Jurassic (Fig. 4). It also implies that neosauropods became widespread and diverse in Middle Jurassic, partly reflecting an increasing shift to habitats and niche differentiation (e.g. coexistence among *Dashanpusaurus* and other non-neosauropodan sauropods with prominent size diversification and morphologic difference). Variations of skull features and associated inferences (e.g. cranial robustness and occlusal relationships of skull anatomy; tooth wear pattern; dietary preferences; snout shape and dental microwear for the feeding strategy; neck length for the browsing height) among different sauropod species have been used to indicate niche partitioning and different resource use strategies (e.g. Whitlock, 2011; D'Emic, 2012, 2013; Wilkinson and Ruxton, 2013; Button et al., 2014, 2017; Mannion et al., 2013, 2021). Within the Lower Shaximiao Formation of Dashanpu, there were typically six sauropod dinosaur genera living in sympatry at any time (Dong et al., 1983; Dong and Tang, 1984; He et al., 1988; Zhang, 1988; Ouyang, 1989; Kuang, 2004; Peng et al., 2005; Jiang et al., 2011). At least two different types of body plans in Dashanpu sauropods: the long-neck species (e.g. *Omeisaurus tianfuensis*; *O. Jiaoi*) and short-neck species (e.g. *Shunosaurus lii*; *Dashanpusaurus dongi*), may indicate different browsing height. Although the teeth of Dashanpu sauropods share with spoon-shaped crown, three morphological types of teeth could be distinguished least: spatulate, narrow-crowned (e.g. *Shunosaurus lii*); spatulate, broad-crowned teeth (e.g. *Omeisaurus tianfuensis*); much robust, broad-crowned teeth (e.g. *Datousaurus bashanensis*) and its potentially distinct implications for food intake. Their morphological and body-size variations may explain the coexistence of these animals and high niche differentiation from the same fossil quarry (SD1, Supplementary figures 3-6). In contrast to the low sauropod diversity in the late Early Jurassic of East Asia, this high niche partitioning hypothesis could be a mechanism driving the diversification of the Dashanpu Middle Jurassic sauropod fauna.

Based on the global and temporal distribution, it would appear that non-titanosauriform macronarians may have a Laurasian and potentially an East Asian origin (Fig. 5). Despite the occasional phylogenetic disagreement, non-titanosauriform macronarians (e.g. the phylogenetic position of *Bellusaurus* in Mannion et al. (2019) and this paper), appear to have a nearly global distribution from Middle Jurassic to Early Cretaceous (Fig. 4). Except for the Bajocian *Dashanpusaurus* from China, other macronarian taxa are from Late Jurassic to Early Cretaceous Asia, Europe, North America, and Africa. However, Moser et al. (2006) claimed to have fragmentary camarasaurid-like material from the Bajocian of India, and *Atlasaurus* is occasionally positioned as the early-diverging macronarian (Bathonian-Callovian) from Morocco (e.g. Woodruff and Foster, 2017). The earliest macronarian and neosauropod thus far identified is *Dashanpusaurus* from the Middle Jurassic (early Bajocian) of China. Macronarians were probably diverse and widespread as early as the early Middle Jurassic.

In both the harsh and relaxed EWP analyses, the MRCA of *Dashanpusaurus/Camarasaurus* and other macronarians is present in Asia and North America. As noted above, the land connection between the two regions was severed in the late Middle Jurassic (Poropat et al., 2016). Thus, the close relationship between Bajocian *Dashanpusaurus* and Late Jurassic *Camarasaurus* spp. are currently best explained as the result of a dispersal event (although a big time gap between the two taxa, there is not any more closely related to either taxon was reported except for the putative macronarian *Atlasaurus* from late Middle Jurassic), as part of the near-global expansion of early-diverging macronarians during the early Middle and early Late Jurassic (Fig. 5). The results outlined above suggest this clade was assembled through a diverse and complex series of biogeographic events: some non-neosauropodan eusauropods and early-diverging neosauropods became widespread across a substantial portion of Pangaea or perhaps globally during the late Early to Middle Jurassic.

5. Conclusions

Our resolution of *Dashanpusaurus dongi* within Macronaria pushes its divergence from Diplodocoidea (within Neosauropoda) back to the early Middle Jurassic. It further suggests the diversity of neosauropods in the Middle Jurassic was substantially higher than previously estimated. The dispersal of the major non-neosauropodan eusauropod and some members of neosauropod lineages occur before the Middle/Late

Jurassic boundary before the fragmentation of Pangaea. The dispersal potentially occurred regionally and globally during the late Early to Middle Jurassic. Although the precise origination time for neosauropods is inconclusive, existing pieces of evidence reinforce that the late Early Jurassic to early Middle Jurassic was a critical phase in sauropod evolution is potentially high rates of morphology, diversification, and distribution.

Acknowledgements

We thank Yu Liu, Xi Shen, and Xiaomei Zhou for preparing specimens at Zigong Dinosaur Museum. We are grateful to Howard J. Falcon-Lang and two anonymous reviewers for the suggestions that improved the earlier version of this manuscript. Thoughtful reviews by Stephen F. Poropat, an anonymous reviewer, and the editor significantly improved the manuscript. This work was supported by grants from the Strategic Priority Research Program of the Chinese Academy of Sciences (Grant No. XDB26000000), the National Natural Science Foundation of China (Grant No. 42288201 and 42102018), and the China Geological Survey (Grant No. DD20221649).

Author contributions

Xin-Xin Ren and Hai-Lu You conceived of, designed, and coordinated the study, collected and interpreted the data, performed the analyses, and drafted the manuscript and figures. Lei Jia interpreted data and critically revised the manuscript. Shan Jiang, Xu-Ri Wang, Guang-Zhao Peng, and Yong Ye participated in collecting the data and providing access to materials. All authors gave final approval for publication and agree to be held accountable for the work performed therein.

References

Averianov, A.O., Zverkov, N.G., 2020. New diplodocoid sauropod dinosaur material from the Middle Jurassic of European Russia. Acta Palaeontologica Polonica 65, doi:10.4202/app.00724.2020

Bell, M.A., Lloyd, G.T., 2015. strap: an R package for plotting phylogenies against stratigraphy and assessing their stratigraphic congruence. Palaeontology 58, 379–389.

BGMRSP (Bureau of Geology and Mineral Resources of Sichuan Province), 1997. Stratigraphy (Lithostratic) of Sichuan Province. China University of Geosciences Press, Wuhan, pp. 1–417 (in Chinese).

Bonaparte, J.F., 1986. The early radiation and phylogenetic relationships of the Jurassic sauropod dinosaurs, based on vertebral anatomy. In: Padian, K. (Eds) The Beginning of the Age of Dinosaurs. Cambridge University Press, UK, pp. 247–258.

Bonaparte, J.F., Heinrich, W.D., Wild, R., 2000. Review of *Janenschia* Wild, with the description of a new sauropod from the Tendaguru beds of Tanzania and a discussion on the systematic value of procoelous caudal vertebrae in the sauropoda. Palaeontographica Abt. A 256, 25–76.

Brusatte, S.L., Benton, M.J., Ruta, M., Lloyd, G.T., 2008. The first 50 Myr of dinosaur evolution: macroevolutionary pattern and morphological disparity. Biology Letters 4, 733–736.

Burnham, K.P., Anderson, D.R., 2002. Model selection and multimodel inference. A practical information - theoretic approach, 2nd edn. Springer, New York, 488.

Button, D.J., Barrett, P.M., Rayfield, E.J., 2017. Craniodental functional evolution in sauropodomorph dinosaurs. Paleobiology 43, 435–462.

Button, D.J., Rayfield, E.J., Barrett, P.M., 2014. Cranial biomechanics underpins high sauropod diversity in resource-poor environments. Proc. R. Soc. B 281, 20142114. http://dx.doi.org/10.1098/rspb.2014.2114

Canudo, J.I., Gasca, J.M., Moreno-Azanza, M., Aurell, M., 2012. New information about the stratigraphic position and age of the sauropod *Aragosaurus ischiaticus* from the Early Cretaceous of the Iberian Peninsula. Geological Magazine 149, 252–263.

Carballido, J.L., Holwerda, F.M., Pol, D., Rauhut, O.W.M., 2017. An Early Jurassic sauropod tooth from Patagonia (Cañadón Asfalto Formation): implications for sauropod diversity. Publicación Electrónica de la Asociación Paleontológica Argentina 17, 50–57.

Carballido, J.L., Sander, P.M., 2013. Postcranial axial skeleton of *Europasaurus* *holgeriholgeri* (Dinosauria, Sauropoda) from the Upper Jurassic of Germany: implications for sauropod ontogeny and phylogenetic relationships of basal Macronaria. Journal of Systematic Palaeontology, 1–50.

CCMSPSB (Compilers of the Continental Mesozoic Stratigraphy and Paleontology of Sichuan Basin), 1982. Continental Mesozoic Stratigraphy and Paleontology of Sichuan Basin. Sichuan People's Publishing House, Chengdu, pp. 1–425 (in Chinese).

Chen, P.J., Li, W.B., Chen, J.H., et al., 1982. Jurassic and Cretaceous fossil sequences of China. Science China B, 558–565.

Cohen, K.M., Finney, S.C., Gibbard, P.L., Fan, J.X., 2013. The ICS International Chronostratigraphic Chart. Episodes 36, 199–204.

Cortés, J.E., Gómez J.J., 2018. The epiclastic barrier-island system of the Early–Middle Jurassic in eastern Spain. Journal of Iberian Geology 44, 257–271.

D'Emic, M.D., 2012. The early evolution of titanosauriform sauropod dinosaurs. Zool J Linn Soc-Lond 166, 624–671.

D'Emic, M.D., Whitlock, J.A., Smith, K.M., Fisher, D.C., Wilson, J.A., 2013. Evolution of high tooth replacement rates in sauropod dinosaurs. PLoS ONE 8, e69235.

Deng, S.H., Lu, Y.Z., Zhao, Y., Fan, R., Wang, Y.D., Yang, X.J., Li, X., Sun, B.N., 2017. The Jurassic palaeoclimate regionalization and evolution of China. Earth Science Frontiers 24, 106–142.

Dercourt, J., Fourcade, E., Cecca, F., et al., 1994. Palaeoenvironment of the Jurassic system in the Western and Central Tethys (Toarcian, Callovian, Kimmeridgian, Tithonian): An overview. Geobios. 27, 625–644.

Dong, Z.M., Tang, Z.L., 1984. Note on a new Mid-Jurassic sauropod (*Datousaurus bashanensis* gen. et sp.nov.) form Sichuan Basin, China. Vertebrata PalAsiatica, 22, 69–75.

Dong, Z.M., Zhou, S.W., Zhang, Y.Z., 1983. The Jurassic dinosaurs of the Sichuan Basin. Palaeontologica Sinica Series C, 23, 1–186.

Goloboff, P.A., Farris, J., Nixon, K.C., 2008. TNT, a free program for phylogenetic analysis. Cladistics 24, 774–786.

Gorscak, E., O’Connor, P.M., 2016. Time-calibrated models support congruency between Cretaceous continental rifting and titanosaurian evolutionary history. Biology Letters 12, 20151047.

Guo, Z.H., Zhao, B., Wu, S., 2000. Jurassic system of Dayi, Chongzhou, Wenchuan and Dujiangyan, Sichuan, Journal of Chengdu University of Technology 27, 31–39.

Haq, B.U., 2017. Jurassic sea-level variations: a reappraisal. Geol. Soc. Am. 28, 4–10.

He, X.L., Li, C., Cai, K.J., 1988. *Omeisaurus tianfuensis.* The Middle Jurassic Dinosaur Fauna from Dashanpu, Zigong, Sichuan: Sauropod Dinosaurs, Volume 4. Sichuan Publishing House of Science and Technology, Chengdu, pp. 1–143

Holwerda, F.M., Evans, M., Liston, J.J., 2019. Additional sauropod dinosaur material from the Callovian Oxford Clay Formation, Peterborough, UK: evidence for higher sauropod diversity. PeerJ 7, e6404.

Jain, S., Abdelhady, A.A., 2020. Paleobiogeography of the Middle Jurassic (Bathonian-Callovian) benthic foraminifera. Marine Micropaleontology doi:10.1016/j.marmicro.2020.101922

Jiang, S., Li, F., Peng, G.Z., Ye, Y., 2011. A new species of Omeisaurus from the Middle Jurassic of Zigong, Sichuan. Vertebrata PalAsiatica 49, 185–194.

Kuang, X.W., 2004. A new Sauropoda from Kaijiang dinosaur fauna in Middle Jurassic beds of North-Eastern Sichuan. In: Sun, J.W., (Eds) Collection of the 90th anniversary of Tianjin Museum of Natural, Tianjin, pp. 1–40.

Li, R.B., Pei, X.Z., Liu, Z.Q., et al., 2010. Basin-Mountain Coupling Relationship of Foreland Basins between Dabashan and Northeastern Sichuan -the Evidence from LA-ICP-MS U-Pb Dating of the Detrital Zircons. Acta Geol. Sin. 84, 1118–1134.

Liao, H.Y., Shen, Y.B., Huang, D.Y., 2014. Micro ornamentations on the carapaces of *Euestheria jingyuanensis* (Crustacea: Spinicaudata) and its biostratigraphic significance. Acta Palaeontologica Sinica 53, 210–216.

Longman, H. A., 1926. A giant dinosaur from Durham Downs, Queensland. Memoirs of the Queensland Museum 8, 183–194.

Luo, L., Qi, J.F., Zhang, M.Z., Wang, K., Han, Y.Z., 2014. Detrital zircon U–Pb ages of Late Triassic–Late Jurassic deposits in the western and northern Sichuan

Basin margin: constraints on the foreland basin provenance and tectonic implications. Internat. J. Earth Sci. 103, 1553–1568.

Maddison, W.P., Maddison, D.R., 2011. Mesquite: a modular system for evolutionary analysis. Version 2.75 edn https://www.mesquiteproject.org/

Manabe, M., Barrett, P.M., Isaji, S., 2000. A refugium for relicts? Nature 404, 953.

Mannion, P.D., Tschopp, E., Whitlock, J.A., 2021. Anatomy and systematics of the diplodocoid *Amphicoelias altus* supports high sauropod dinosaur diversity in the Upper Jurassic Morrison Formation of the USA. R. Soc. Open Sci. 8, 210377. https://doi.org/10.1098/rsos.210377

Mannion, P.D., Upchurch, P., Barnes, R.N., Mateus, O., 2013. Osteology of the Late Jurassic Portuguese sauropod dinosaur *Lusotitan atalaiensis* (Macronaria) and the evolutionary history of basal titanosauriforms. Zool J Linn Soc-Lond 168, 98– 206.

Mannion, P.D., Upchurch, P., Hutt, S., 2011. New rebbachisaurid (Dinosauria: Sauropoda) material from the Wessex Formation (Barremian, Early Cretaceous), Isle of Wight, United Kingdom. Cretaceous Research 32, 774–780.

Mannion, P.D., Upchurch, P., Schwarz, D.A., Wings, O., 2019. Taxonomic affinities of the putative titanosaurs from the Late Jurassic Tendaguru Formation of Tanzania: phylogenetic and biogeographic implications for eusauropod dinosaur evolution. Zoological Journal of the Linnean Society 99, 1–126.

Matzke, N.J., 2013. Probabilistic historical biogeography: new models for founder-event speciation, imperfect detection, and fossils allow improved accuracy and model-testing. Frontiers of Biogeography 5, 242–248.

Matzke, N.J., 2014. Model selection in historical biogeography reveals that founder-event speciation is a crucial process in island clades. Systematic Biology 63, 951–970.

Marcinowski, R., Gasiński, A., 2002. Cretaceous biogeography of epicratonic Poland and Carpathians. In: Michalik J., (Eds). Tethyan/Boreal Cretaceous Correlation. Mediterranean and Boreal Cretaceous paleobiogeographic areas in Central and Eastern Europe. VEDA, Bratislava, pp. 1–161.

Marsh, O.C., 1878. Principal characters of American Jurassic dinosaurs. American Journal of Science 3, 411–416.

Mo, J., 2013. Topics in Chinese dinosaur paleontology: *Bellusaurus sui*. Henan Science and Technology Press, Zhengzhou, pp. 1–155.

Mocho, P., Royo-Torres, R., Ortega, F., 2014. Phylogenetic reassessment of *Lourinhasaurus alenquerensis*, a basal Macronaria (Sauropoda) from the Upper Jurassic of Portugal. Zoological Journal of the Linnean Society 170, 875–916.

Monbaron, M., Russell, D.A., Taquet, P., 1999. *Atlasaurus imelakei* n.g., n.sp., a brachiosaurid-like sauropod from the Middle Jurassic of Morocco. Palaeontology/Paléontologie 329, 519–526.

Moore, A.J., Upchurch, P., Barrett, P.M., et al., 2020. Osteology of *Klamelisaurus gobiensis* (Dinosauria, Eusauropoda) and the evolutionary history of Middle–

Late Jurassic Chinese sauropods. Journal of Systematic Palaeontology 21, 1–95.

Moser, M., Mathur, U.B., Fürsich, F.T., et al., 2006. Oldest camarasauromorph sauropod (Dinosauria) discovered in the Middle Jurassic (Bajocian) of the Khadir Island, Kachchh, western India. Paläontologische Zeitschrift 80, 34–51.

Nair, J.P., Salisbury, S.W., 2012. New anatomical information on Phoetosaurus brownei Longman, 1926, a gravisaurian sauropodomorph dinosaur from the Middle Jurassic of Queensland, Australia. Journal of Vertebrate Paleontology 32, 369–394.

Nielsen, L.H., Petersen, H.I., Dybkjær, K., et al., 2010. Lake-mire deposition, earthquakes and wildfires along a basin margin fault; Rønne Graben, Middle Jurassic, Denmark. Palaeogeography, Palaeoclimatology, Palaeoecology 292, 103–126.

Ouyang, H., 1989. A new sauropod from Dashanpu, Zigong Co., Sichuan Province (*Abrosaurus dongpoensis* gen. et sp. nov.). Zigong Dinosaur Museum Newsletter 2, 10–14.

Peng, G.Z., Ye, Y., Gao, Y.H., et al., 2005. Jurassic Dinosaur Faunas in Zigong. Sichuan People's Publishing House, Chengdu, pp. 1-–236.

Poropat, S.F., Mannion, P.D., Upchurch, P., et al., 2016. New Australian sauropods shed light on Cretaceous dinosaur palaeobiogeography. Scientific Reports 6, 34467.

Poropat, S.F., Frauenfelder, T.G., Mannion, P.D., Rigby, S.L., Pentland, A.H., Sloan, T., Elliott, D.A., 2022. Sauropod dinosaur teeth from the lower Upper Cretaceous Winton Formation of Queensland, Australia and the global record of early titanosauriforms. R. Soc. Open Sci. 9, 220381. doi:10.1098/rsos.22038

Qian, T., Liu, S.F., Wang, Z.X., Li, W.P., Chen, X.L., 2016. A detrital record of continent-continent collision in the Early-Middle Jurassic foreland sequence in the northern Yangtze foreland basin, South China. J. Asian Earth Sci. 131, 123–137.

R Core Development Team., 2015. R: a language and environment for statistical computing. v. 3.3.2. Vienna, Austria: R Foundation for Statistical Computing. Available at: http://www.R-project.org/.

Remes K, Ortega F, Fierro I, Joger U, Kosma R, et al., 2009. A new basal sauropod dinosaur from the Middle Jurassic of Niger and the early evolution of Sauropoda. PLoS ONE 4, e6924. doi:10.1371/journal.pone.0006924

Ren, X.X., Huang, J.D., You, H.L., 2018. The second mamenchisaurid dinosaur from the Middle Jurassic of Eastern China. Historical Biology doi:10.1080/08912963.2018.1515935

Ren, X.X., Jiang, S., Wang, X.R., Peng, G.Z., Ye, Y., King, L., You, H.L., 2022. Osteology of *Dashanpusaurus dongi* (Sauropoda: Macronaria) and new evolutionary evidence from Middle Jurassic Chinese sauropods. Journal of Systematic Palaeontology doi:10.1080/14772019.2022.2132886

Ren, X.X., Sekiya, Y., Wang, T., Yang, Z.W., You, H.L., 2020. A revision of the referred specimen of *Chuanjiesaurus anaensis* Fang et al., 2000: a new early branching mamenchisaurid sauropod from the Middle Jurassic of China. Historical Biology doi:10.1080/08912963.2020.1747450

Royo-Torres, R., Upchurch, P., Mannion, P.D., et al., 2014. The anatomy, phylogenetic relationships and stratigraphic position of the Tithonian–Berriasian Spanish sauropod dinosaur *Aragosaurus ischiaticus*. Zoological Journal of the Linnean Society 171, 623–655.

Ruban, D.A., 2007. Jurassic transgressions and regressions in the Caucasus (northern Neotethys Ocean) and their influences on the marine biodiversity. Palaeogeogr Palaeoclimatol Palaeoecol 251, 422–436

Russell, D.A., 1993. The role of Central Asia in dinosaurian biogeography. Can. J. Earth Sci. 30, 2002–2012.

Scotese, C.R., 2014. Atlas of Jurassic Paleogeographic Maps, PALEOMAP Atlas for ArcGIS, volume 4, The Jurassic and Triassic, Maps 32–42, Mollweide Projection, PALEOMAP Project, Evanston, IL.

Shen, Y.B., 2003. Conchostracan faunas of Jurassic. In: Deng, S.H., Yao, Y. M., Ye, D.Q. (Eds), Jurassic system in the North of China, Volume I, Stratum Introduction. Petroleum Industry Press, Beijing. pp. 50–58.

Shen, Y.B., 2004. Conchostraca. In Yumen Oilfield Company, PetroChina Co. Ltd., Nanjing Institute of Geology and Palaeontology and Chinese Academy of Sciences (Eds), Cretaceous and Jurassic Stratigraphy and Environment of the

Chaoshui and Yabulai Basins, NW China. University of Science and Technology of China Press, Beijing, pp. 54–55.

Shen, Y.B., 2010. Conchostraca fauna. In Deng, S.H. (Eds), The Jurassic system of Northern Xinjiang, China. Contributions to the 8th International Congress on the Jurassic System. University of Science and Technology of China Press, Beijing, pp. 179–184.

Tiss, L., Trabelsi, K., Kamoun, F., et al., 2019. Middle Jurassic charophytes from southern Tunisia: Implications on evolution and paleobiogeography. Review of Palaeobotany and Palynology 263, 65–84.

Upchurch, P., Mannion, P.D., Taylor, M.P., 2015. The anatomy and phylogenetic relationships of *'Pelorosaurus' becklesii* (Neosauropoda, Macronaria) from the Early Cretaceous of England. PLoS ONE 10, e0125819.

Upchurch, P., Mannion, P.D., Xu, X., Barrett, P.M., 2021. Reassessment of the Late Jurassic eusauropod dinosaur *Hudiesaurus sinojapanorum* Dong, 1997, from the Turpan Basin, China, and the evolution of hyper-robust antebrachia in sauropods, Journal of Vertebrate Paleontology doi:10.1080/02724634.2021.1994414

Upchurch, P., Tomida, Y., Barrett, P.M., 2004. A new specimen of *Apatosaurus ajax* (Sauropoda: Diplodocidae) from the Morrison Formation (Upper Jurassic) of Wyoming, USA. National Science Museum Monographs 26, 1–107.

Vidal, D., Mocho, P., Aberasturi, A., Sanz, J. L., Ortega, F., 2020. High browsing skeletal adaptations in *Spinophorosaurus* reveal an evolutionary innovation in sauropod dinosaurs. Scientific Reports 10, doi:10.1038/s41598-020-63439-0.

Wang, J., Ye, Y., Pei, R., Tian, Y.M., Feng, C.Q., Zheng, D.R., Chang, S.C., 2018. Age of Jurassic basal sauropods in Sichuan, China: a reappraisal of basal sauropod evolution. Geol. Soc. Am. Bull. 130, 1493–1500.

Wang, Y.D., Fu, H., Xie, P., Huang, S., Li, K., Li, G., Liu Z.S., Yu, J.X., Pan, Y.H., Tian, N., Jiang, Z.K., 2010. The terrestrial Triassic and Jurassic Systems in the Sichuan Basin, China. University of Science and Technology Press, Hefei, pp1–216.

Whitlock, J.A., 2011. Inferences of diplodocoid (Sauropoda: Dinosauria) feeding behavior from snout shape and microwear analyses. PLoS ONE 6, e18304.

Wilkinson, D.M., Ruxton, G.D., 2012. High C/N ratio (not low-energy content) of vegetation may have driven gigantism in sauropod dinosaurs and perhaps omnivory and/or endothermy in their juveniles. Functional Ecology 27, 131–135.

Wilson, J.A., Sereno, P.C., 1998. Early evolution and higherlevel phylogeny of sauropod dinosaurs. Soc Vert Paleontol Mem. 5, 1–68.

Wilson, J.A., Upchurch, P., 2009. Redescription and reassessment of the phylogenetic affinities of *Euhelopus zdanskyi* (Dinosauria: Sauropoda) from the Early Cretaceous of China. Journal of Systematic Palaeontology 7, 199–239.

Woodruff, D.C., Foster, J.R., 2017. The first specimen of *Camarasaurus* (Dinosauria: Sauropod) from Montana: The northernmost occurrence of the genus. PLoS ONE 12, e0177423.

Xin, C.L., Wang, L.H., Du, B.X., 2018. Cuticles and spores in situ of *Coniopteris hymenophylloides* from the Middle Jurassic in Gansu, Northwestern China. Acta Geologica Sinica (English Edition) 92, 904–914.

Xing, L.D., Miyashita, T., Zhang, J.P., et al., 2015. A new sauropod dinosaur from the Late Jurassic of China and the diversity, distribution, and relationships of mamenchisaurids. Journal of Vertebrate Paleontology 35, e889701.

Xu, X., Upchurch, P., Mannion, P.D., et al., 2018. A new Middle Jurassic diplodocoid suggests an earlier dispersal and diversification of sauropod dinosaurs. Nature communication 9, 2700.

Yang, X.H., 1987. Jurassic plants from the Lower Shaximiao Formation of Rongxian, Sichuan. Bull. Chengdu Inst. Geol. M. R., Chinese Acad. Geol. Sci. 8, 1–16.

You, S.S., Li, Z.J., Li, Y.B., 2019. The stratigraphical characteristics and sedimentary environment of dinosaur fossils in Lingwu, Ningxia. Geological Journal of Sichuan 39, 31–35.

Zhang, H.L., Yang, W.G., Zhu, L.D., Lu, Z.Y., Su, X., Li C.Z., 2019. Zircon U-Pb age, geochemical characteristics and geological significance of highly differentiated S-Type granites in the South Lhasa Block. Mineralogy and Petrology 39, 52–62.

Zhang, W.T., Cheng, P. J., Shen, Y. B., 1976. Fossil Conchostracans of China. Science Press, Beijing, pp. 172–174

Zhang, Y.H., 1988. *Shunosaurus lii*. The Middle Jurassic Dinosaur Fauna from Dashanpu, Zigong, Sichuan: Sauropod Dinosaurs, Volume 3. Sichuan Publishing

House of Science and Technology, Chengdu, pp. 1–89.

Zhou, Y., Dai, H., Yu, H., et al., 2021. Zircon geochronology of the new dinosaur fauna in the Middle Jurassic lower Shaximiao Formation in Chongqing, SW China. Palaeogeography, Palaeoclimatology, Palaeoecology https://doi.org/ 10.1016/j.palaeo.2022.110894

Zatoń, M., 2011. Diversity dynamics of ammonoids during the latest Bajocian and Bathonian (Middle Jurassic) in the epicratonic Polish Basin. Palaeobio 91, 89–99.

Zatoń, M., Marynowski, L., 2006. Ammonite fauna from uppermost Bajocian (Middle Jurassic) calcitic concretions from the Polish Jura - biogeographical and taphonomical implications. Geobios 39, 426–442.

Zatoń, M., Taylor, P.D., 2009. Middle Jurassic cyclostome bryozoans from the Polish Jura. Acta Palaeontol Polon 54, 267–288.

Zohdi, A., Immenhauser, A., Rabbani, J., 2021. Middle Jurassic evolution of a northern Tethyan carbonate ramp (Alborz Mountains, Iran). Sedimentary Geology 416, 105866.

Zong, H., Shi, H., 1997. The Jurassic System of Dujiangyan, Pengzhou and Shifang, Sichuan. Journal of Stratigraphy 21, 192-202.

Table 1. Summary of results and statistical comparisons between the six biogeographic models applied in the BioGeoBEARS analyses for the equal weights agreement subtree. The

‘Ratio’ in the AIC analyses is the ratio of the AIC weight for the +J version of the same model (e.g. DEC+J/DEC). An asterisk (*) marks those models that are regarded as best fitting the data in each analysis.

Analysis	Model	LnL	Ln likelihood ratio		AIC Analysis		
			D statistic	*P* value	AIC	AIC wt	Ratio
Relaxed	DEC	-294.8			593.7	1.50e^{-6}	
	DEC+J	-280.5	28.78	8.10e^{-08}	566.9	1.00	1.50e^{5}
	DIVALIKE	-359.1			722.2	3.10e^{-23}	
	DIVALIKE+J	-306.3	105.7	8.70e^{-25}	618.5	1.00	3.25e^{22}
	BAYAREALIKE	-311.8			627.5	1.10e^{-16}	
	*BAYAREALIKE+J	-274	75.47	3.70e^{-18}	554.1	1.00	8.97e^{15}
Harsh	DEC	-297.3			598.5	1.00e^{-4}	
	DEC+J	-287.1	20.38	6.40e^{-06}	580.1	1.00	9.78e^{3}
	DIVALIKE	-360.3			724.6	4.70e^{-18}	
	DIVALIKE+J	-319.4	81.8	1.50e^{-19}	644.8	1.00	2.13e^{17}
	BAYAREALIKE	-313.1			630.1	5.00e^{-14}	
	*BAYAREALIKE+J	-281.4	63.37	1.80e^{-15}	568.9	1.00	2.01e^{13}

Fig. 1. Geological map showing the Dashanpu dinosaur fauna location, and generalized stratigraphic section of Jurassic in Sichuan Basin. Silhouette showing preserved elements in skeletal reconstruction.

Fig. 2. Autapomorphies from the dorsal and left humerus materials of *Dashanpusaurus dongi.* A and C, D1-2 and D6 in anterior view; B and D, D1-2 and D6 in lateral view; E and F, left humerus in anterior and distal view. *Abbreviations*: **AL**, accessory lamina contacting the perzygodiapophyseal lamina and paraodiapophyseal lamina; **ap**, accessory process; **CPRL**, centroprezygapophyseal lamina; **di**, diapophysis; **dpc**, deltopectoral crest; **EPRL**, epipophyseal-prezygapophyseal lamina; **IE**, internal excavation; **lc**, lateral condyle; **mc**, medial condyle; **nsp**, neural spine; **pa**, parapophysis; **PCDL**, posterior

centrodiapophyseal lamina; **pf**, lateral pneumatic fossa; **PODL**, postzygodiapophyseal lamina; **poz**, postzygapophysis; **PRDL**, prezygodiapophyseal lamina; **prz**, prezygapophysis; **SPRL**, spinoprezygapophyseal lamina. Scale bars represent 5cm for a-d and 10cm for e-f.

Fig. 3. Time-calibrated phylogenetic agreement subtree, based on equal weights analysis of the main dataset. Agreement subtree produced in TNT. Strict consensus of 3 MPTs (TL= 1387 steps) from phylogenetic analysis (85 taxa, 400 characters). The data matrix follows Ren et al. (2020), with the addition of 14 character codings. All somphospondylans have been combined into a single lineage (See Supplement for the full version of equal-weights and extended implied-weights, and separated OTUs parsimony analysis results). *Abbreviations*: **AF**, Asia - Africa; **AN**, Asia - North America; **AS**, Asia - South America; **AFN**, Asia - Africa - North America; **ANS**, Asia, North America - South America; **AS**, Asia - South America; **MRCA**, the most common ancestor. Black-colored pie charts represent the possible regions of MRCA in harsh analysis; White-colored pie charts represent the possible regions of MRCA in relaxed analysis.

Fig. 4. Paleogeographic reconstruction showing the main Middle Jurassic sauropod faunas discussed in the text. Palaeogeographic reconstruction of 170Ma from PALEOMAP (Scotese, 2014). Sauropods in blue represent the non-neosauropodan eusauropods; sauropods in red represent the macronarian; sauropods in yellow

represent the diplodocoids. *Abbreviations*: **Aal**, Aalenian; **Baj**, Bajocian; **Bat**, Bathonian; **Cal**, Callovian; **Fm.**, Formation.

Fig. 5. Paleogeographic reconstructions at ~170Ma (a) and ~150 Ma (b). A-I (Red, Macro), locations of *Dashanpusaurus* (A), *Bellusaurus* (B), *Europasaurus* (C), *Aragosaurus* (D) and *Galveosaurus* (E), *Lourinhasaurus* (F), *Camarasaurus* (G), *Tehuelchesaurus* (H), and *Janenschia* (I) faunas; J-R (Yellow, Dipl), locations of *Lingwulong* (J), *Atlasaurus* (K), *Haplocanthosaurus* (L), *Diplodocid* (M), *Barosaurus* (N), *Apatosaurus* (O), *Suwasswa* (P), *Brachytrachelopan* (Q), and *Dicraeosaurus* (R) faunas palaeogeographic reconstruction of 170Ma and 150Ma from Ancient Earth Globe (https://dinosaurpictures.org/ancient-earth#170).

Declaration of interests

The authors declare that they have no known competing financial interests or personal relationships that could have appeared to influence the work reported in this paper.

Highlights

- First phylogenetic analysis with the latest datasets confirms that *Dashanpusaurus dongi* lies within Neosauropoda (as an early-diverging macronarian) as one of the earliest neosauropods.
- A new geochronological study on the bottom of the Lower Shaximiao Formation suggests that the age of *Dashanpusaurus dongi* belongs to Bajocian.
- Neosauropods may achieved a global distribution at least in the early Middle

Jurassic while Pangaea was still a coherent landmass.

- High niche partitioning might partly explain the mechanisms driving the diversification of the Dashanpu Middle Jurassic sauropod fauna.

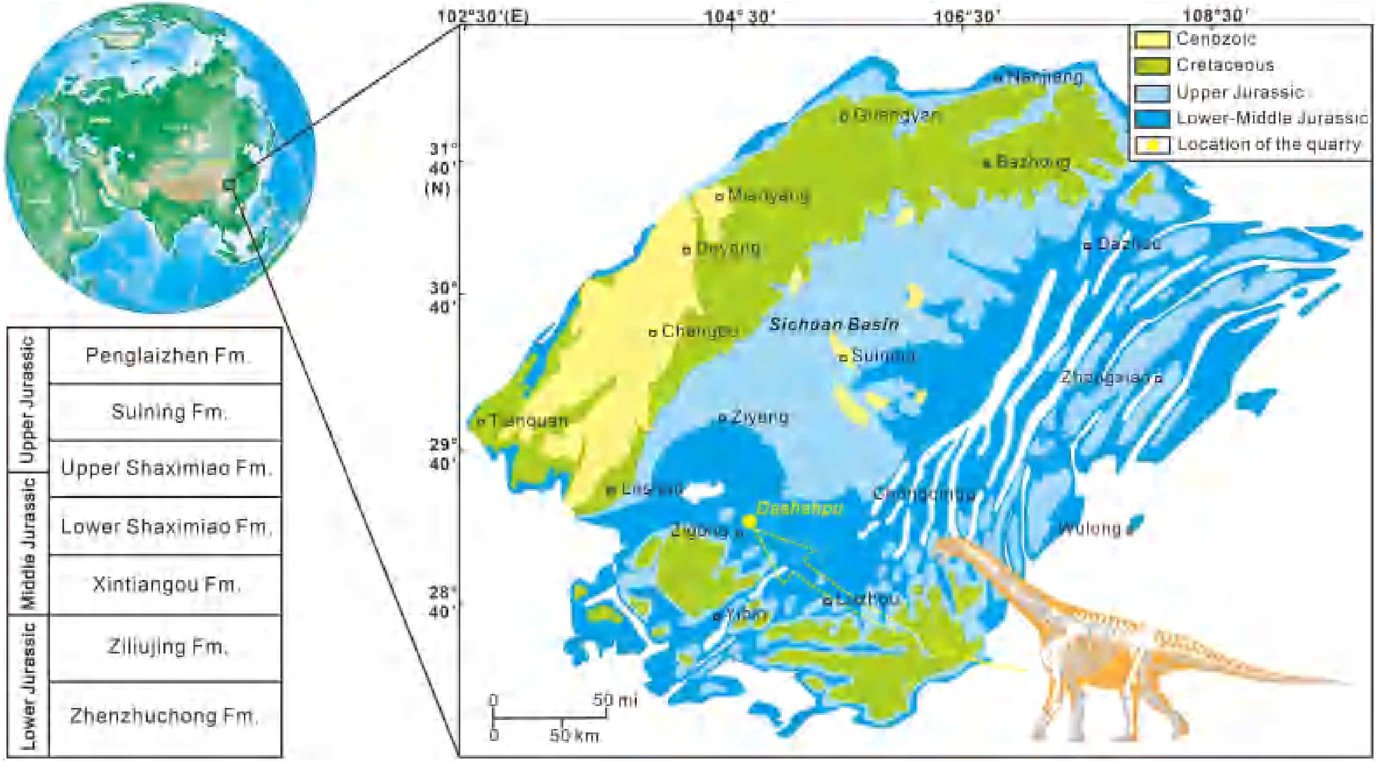

102°30'(E)
104° 30'
106°30'
108°30'
31° 40' (N)
30° 40'
29° 40'
28° 40'
Cenozoic
Cretaceous
Upper Jurassic
Lower-Middle Jurassic
Location of the quarry
Nanjiang
Guangyuan
Bazhong
Mianyang
Deyang
Dazhou
Chengdu
Sichuan Basin
Suining
Ziyang
Tianquan
Leshan
Chongqing
Dashanpu
Zigong
Wulong
Luzhou
Yibin
0
50 mi
0
50 km
Upper Jurassic
Middle Jurassic
Lower Jurassic
Penglaizhen Fm.
Suining Fm.
Upper Shaximiao Fm.
Lower Shaximiao Fm.
Xintiangou Fm.
Ziliujing Fm.
Zhenzhuchong Fm.

Figure 1

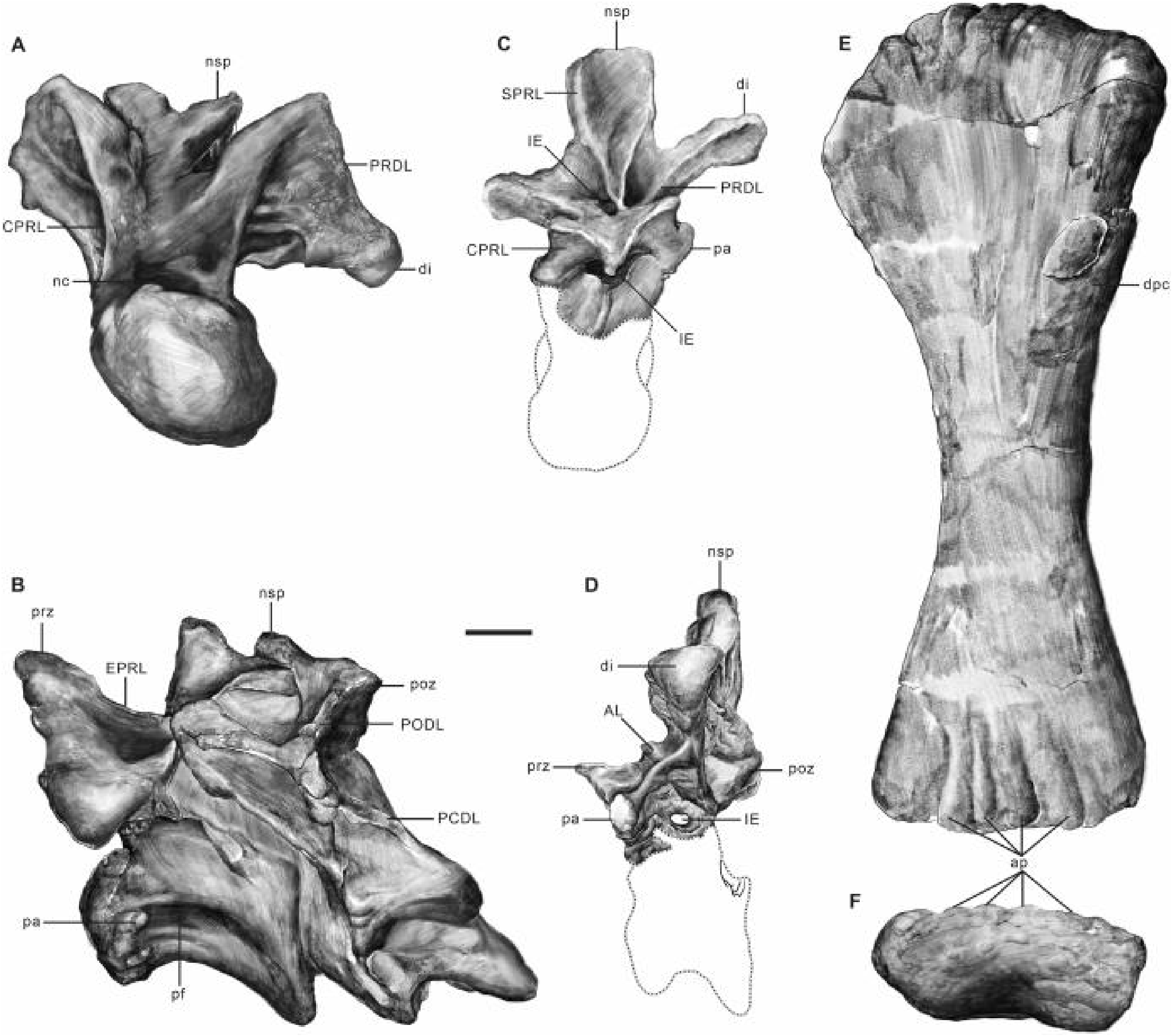
A
nsp
PRDL
CPRL
nc
di
C
nsp
SPRL
di
IE
PRDL
CPRL
pa
IE
E
dpc
B
nsp
prz
EPRL
poz
PODL
PCDL
pa
pf
D
nsp
di
AL
prz
poz
pa
IE
ap
F

Figure 2

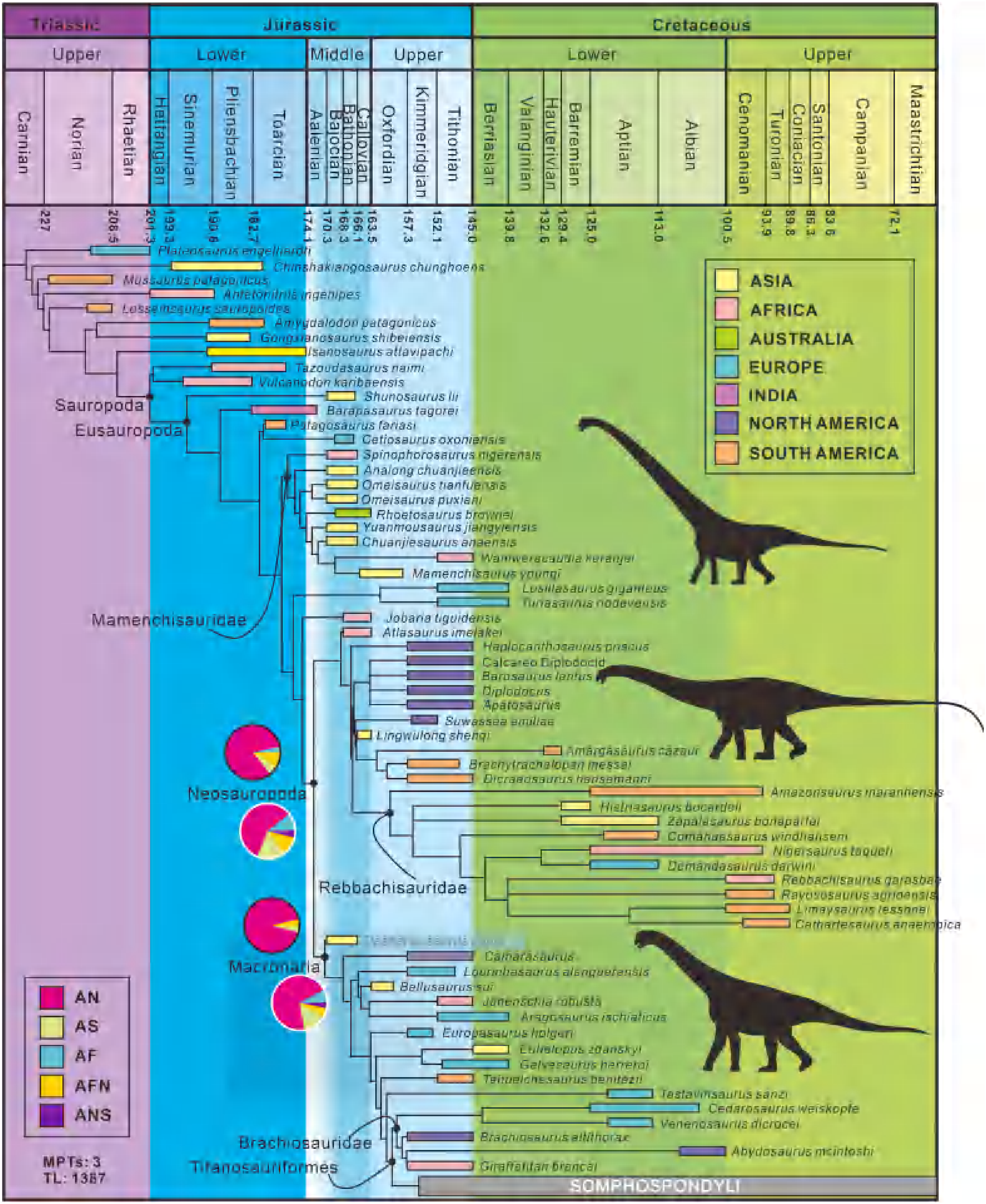

Triassic
Jurassic
Cretaceous
Upper
Lower
Middle
Upper
Lower
Upper
Carnian
Norian
Rhaetian
Hettangian
Sinemurian
Pliensbachian
Toarcian
Aalenian
Bajocian
Bathonian
Callovian
Oxfordian
Kimmeridgian
Tithonian
Berriasian
Valanginian
Hauterivian
Barremian
Aptian
Albian
Cenomanian
Turonian
Coniacian
Santonian
Campanian
Maastrichtian
227
208.5
201.3
199.3
190.8
182.7
174.1
170.3
168.3
166.1
163.5
157.3
152.1
145.0
139.8
132.6
129.4
125.0
113.0
100.5
93.9
89.8
86.3
83.6
72.1
ASIA
AFRICA
AUSTRALIA
EUROPE
INDIA
NORTH AMERICA
SOUTH AMERICA
Mussaurus patagonicus
Antetonitrus ingenipes
Amygdalodon patagonicus
Tazoudasaurus naimi
Vulcanodon karibaensis
Shunosaurus lii
Barapasaurus tagorei
Patagosaurus fariasi
Cetiosaurus oxoniensis
Spinophorosaurus nigerensis
Analong chuanjieensis
Omeisaurus tianfuensis
Omeisaurus puxiani
Rhoetosaurus brownei
Yuanmousaurus jiangyiensis
Chuanjiesaurus anaensis
Mamenchisaurus youngi
Losillasaurus giganteus
Turiasaurus riodevensis
Jobaria tiguidensis
Atlasaurus imelakei
Haplocanthosaurus priscus
Calcareo Diplodocid
Barosaurus lentus
Diplodocus
Apatosaurus
Suwassea emiliae
Lingwulong shenqi
Amargasaurus cazaui
Brachytrachelopan mesai
Dicraeosaurus hansemanni
Amazonsaurus maranhensis
Histriasaurus boscarollii
Zapalasaurus bonapartei
Comahuesaurus windhauseni
Nigersaurus taqueti
Demandasaurus darwini
Rebbachisaurus garasbae
Rayososaurus agrioensis
Limaysaurus tessonei
Cathartesaura anaerobica
Camarasaurus
Lourinhasaurus alenquerensis
Bellusaurus sui
Janenschia robusta
Aragosaurus ischiaticus
Europasaurus holgeri
Euhelopus zdanskyi
Galvesaurus herreroi
Tehuelchesaurus benitezii
Tastavinsaurus sanzi
Cedarosaurus weiskopfae
Venenosaurus dicrocei
Brachiosaurus altithorax
Abydosaurus mcintoshi
Giraffatitan brancai
SOMPHOSPONDYLI
Sauropoda
Eusauropoda
Mamenchisauridae
Neosauropoda
Rebbachisauridae
Macronaria
Brachiosauridae
Titanosauriformes
AN
AS
AF
AFN
ANS
MPTs: 3
TL: 1387

Figure 3

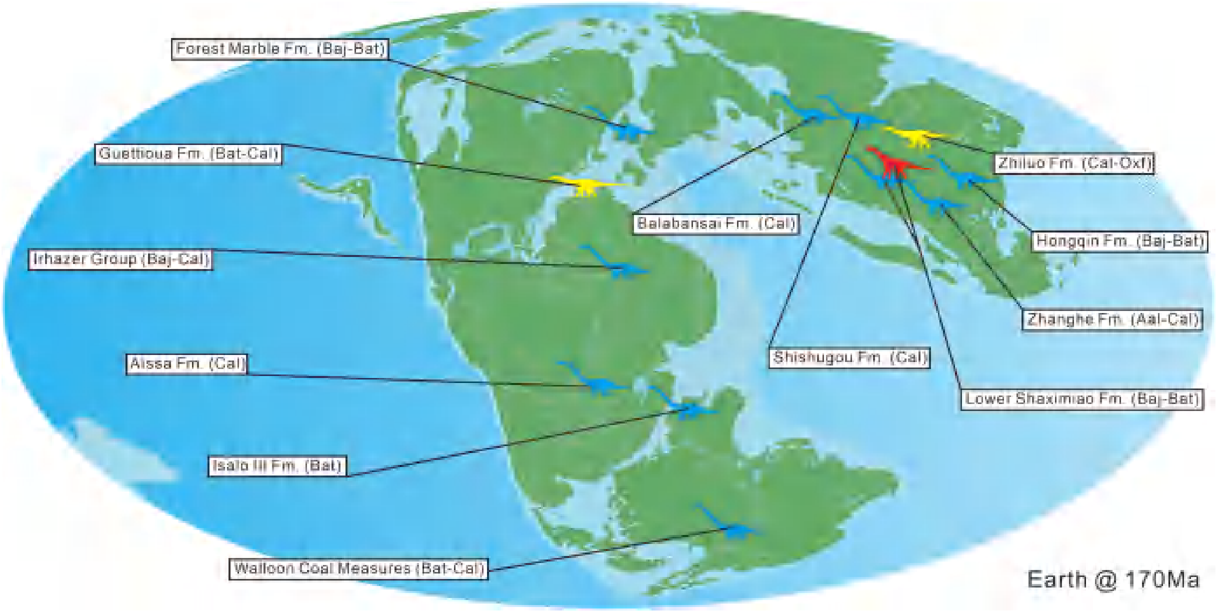
Forest Marble Fm. (Baj-Bat)
Guettioua Fm. (Bat-Cal)
Irhazer Group (Baj-Cal)
Aissa Fm. (Cal)
Isalo III Fm. (Bat)
Walloon Coal Measures (Bat-Cal)
Balabansai Fm. (Cal)
Zhiluo Fm. (Cal-Oxf)
Hongqin Fm. (Baj-Bat)
Zhanghe Fm. (Aal-Cal)
Shishugou Fm. (Cal)
Lower Shaximiao Fm. (Baj-Bat)
Earth @ 170Ma

Figure 4

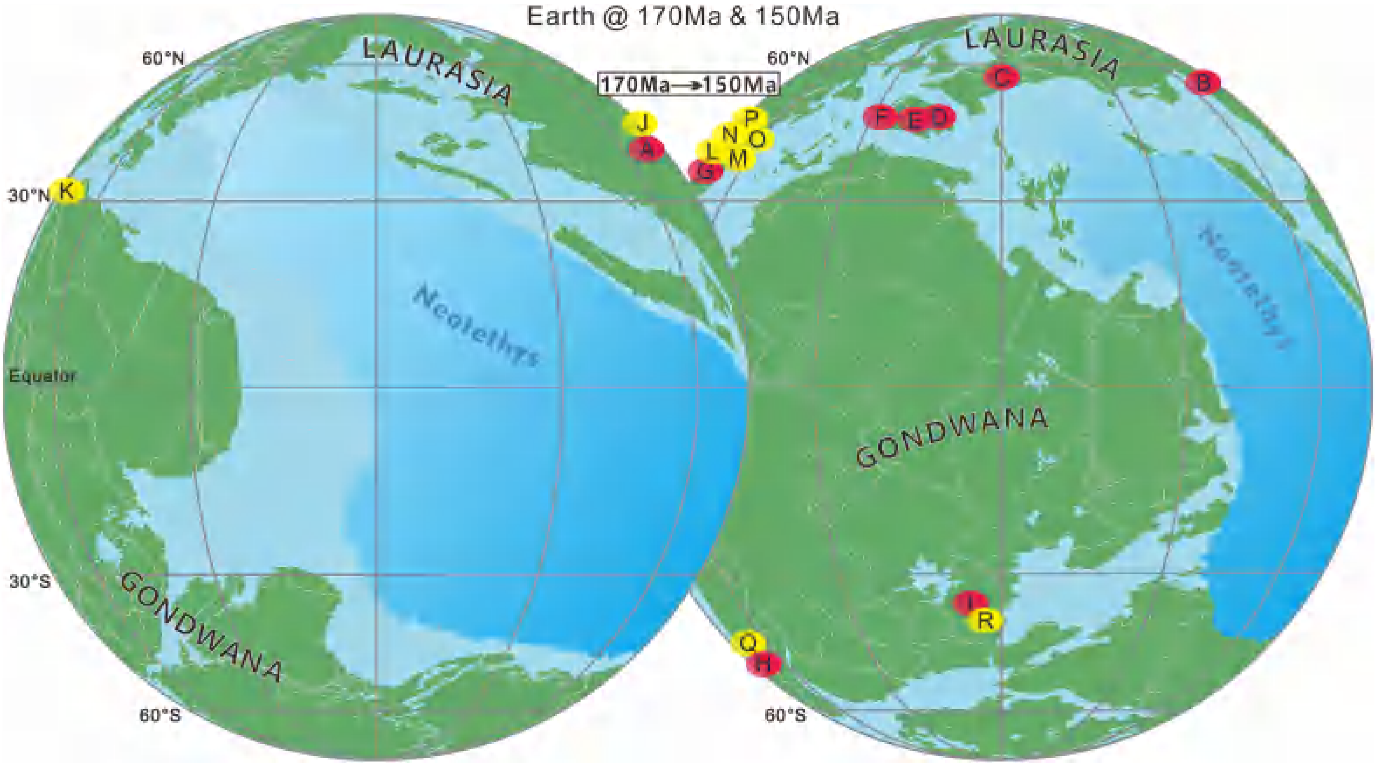
Earth @ 170Ma & 150Ma
170Ma→150Ma
LAURASIA
LAURASIA
60°N
60°N
30°N
Equator
30°S
60°S
60°S
Neotethys
Neotethys
GONDWANA
GONDWANA
A
B
C
D
E
F
G
H
I
J
K
L
M
N
O
P
Q
R

Figure 5